



# Growth, Spectral, Optical, Dielectric, Laser Damage Threshold and Second Harmonic Generation studies of L-Threonine single crystals for Potential nonlinear optical applications

N Mahalakshmi<sup>1</sup>, M Parthasarathy<sup>2\*</sup>

<sup>1,2</sup> Department of Physics, School of Basic Sciences, Vels Institute of Science, Technology and Advanced Studies, Pallavaram, Chennai-600 117, Tamil Nadu, India.

\*Corresponding author E mail: mps2k7@gmail.com (M. Parthasarathy)

---

## Abstract

Slow evaporation solution growth technique was employed to grow an optical single crystals of L-Threonine using water as solvent. It crystalizes in an orthorhombic system with space group  $P2_12_12_1$  was confirmed by single crystal X-ray diffraction. FT-IR spectral analysis verified the various functional groups present in the grown crystal. Optical characteristics were evaluated using UV-Vis-NIR analysis, it was observed with an optical band gap of 5.04 eV and the cut-off wavelength at 232 nm. The Urbach energy of the grown crystal was analysed and it appears to be minimum, which indicates that the L-Threonine has good crystallinity and Steepness parameter, Electron-phonon interaction energy were estimated. Optical properties such as extinction coefficient, optical conductivity and refractive index were measured in terms of photon energy and wavelength. Photoluminescence analysis of the material reveals great structural perfection of L-Threonine, confirms the emission of blue fluorescence. The laser damage threshold value was tested and it was calculated as 50.85  $\text{GW}/\text{cm}^2$  for 1064nm wavelength of Nd:YAG laser radiation. The dielectric permittivity ( $\epsilon'$ ) as a function of frequency was measured. The electronic polarizability ( $\alpha$ ) of the title crystal was calculated. Second Harmonic Generation (SHG) was tested by Kurtz-Perry powder technique and efficiency compared to standard KDP. This result indicates that the material has various NLO, photonic and optoelectronic device applications.

**Keywords:** Single crystal growth, Photoluminescence, Laser Damage Threshold, Dielectric studies and Second Harmonic Generation (SHG).

---

## 1. Introduction

A nonlinear optical effect is the interaction of an electromagnetic field of high intensity laser light with a material. Materials with large nonlinear optical susceptibilities are of importance in optoelectronics, where they are used in the construction of the optical analogues of the circuit elements such as modulators, amplifiers, rectifiers, switches, and so forth, of conventional electronics. Some organic materials have exceptionally large nonlinear susceptibilities, the origins of which can be tracked back to the molecular electronic properties and in the recent years, a great deal of effort has been expanded on their identification and development [1–3]. The non-linear optical properties of large organic

molecules have been subjected into extensive theoretical and experimental investigations during the past two decades for generating the second harmonic frequency, plays an important role in the domain of optoelectronics and photonics [4-5]. Many optically active amino acids show highly efficient optical second harmonic generation (SHG) and are promising candidates for coherent blue-green laser generation and frequency doubling applications. Moreover, amino acids such as L-alanine, L-histidine, and L-threonine have special features such as molecular chirality, wide transparency in the visible and UV ranges, and zwitterionic character. The first feature forces the molecule to crystallize in a noncentrosymmetric space group, which is an essential criterion for a SHG material and the last feature paved the way for possessing high electro optic parameters and good mechanical and thermal strength of the crystals. Among these compounds, L-threonine is an important amino acid which has an SHG efficiency higher than that of many amino acids and their family crystals. The compound crystallizes in the noncentric space group  $P2_12_12_1$  of an orthorhombic system. In this connection the authors grow the title crystals by low temperature solution growth technique using water as a solvent at room temperature and later the as grown crystal was subjected into characterization studies like, optical studies, electrical studies, laser damage threshold and Second Harmonic Generation (SHG).

## 2. Experiment

### 2.1 Single crystal growth

The commercial analytical reagent grade L-Threonine from SRL (pure 99%) was purchased and purified by repeated recrystallization process using water as solvent. Slow evaporation technique was used to grow the crystal under room temperature. The solvent was taken in a beaker and the purified material was added gradually with continuous stirring for 3 hrs to get the saturation. The saturated solution was filtered using whatman filter paper. The filtered solution was poured in a beaker and kept in an undisturbed position for slow evaporation. Transparent good quality single crystals of various sizes were harvested from mother solution after a time span of 40 days. The as grown single crystals are shown in Fig.1

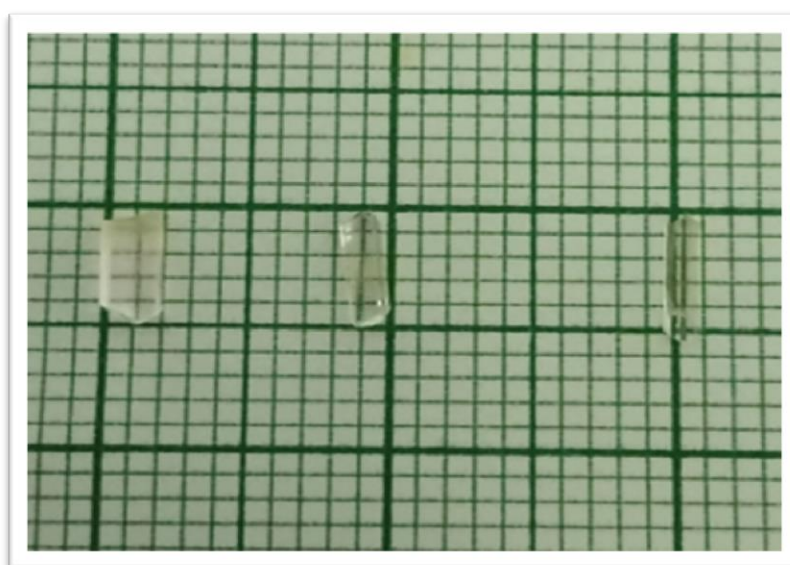


**Fig. 1 As grown single crystals of L-Threonine**

### 3. Results and Discussions

#### 3.1. Single Crystal X-ray Diffraction analysis

The unit cell dimensions and the space group of L-Threonine were obtained using Bruker Kappa single crystal X-ray diffractometer. The crystallographic information of the title crystal is presented in Table 1. The obtained lattice parameter values are well matched with reported literature [6].

**Table. 1 Crystallographic details of L-Threonine**

Molecular Formula	C <sub>4</sub> H <sub>9</sub> NO <sub>3</sub>
Unit cell parameters	$a = 5.18 (2) \text{ \AA}$ , $b = 7.76 (3) \text{ \AA}$ and $c = 13.67 (6) \text{ \AA}$ $\alpha = \beta = \gamma = 90^\circ$
Crystal System	Orthorhombic
Space group	P2 <sub>1</sub> 2 <sub>1</sub> 2 <sub>1</sub>
Cell volume	549 (7) $\text{\AA}^3$

#### 3.2. Fourier Transform Infrared Spectroscopy (FT-IR) Analysis

FT-IR spectrum of L-Threonine were recorded at room temperature in the frequency range 400–4000  $\text{cm}^{-1}$  using BRUKER 66V FT-IR spectrometer, is shown in Fig. 2. In the FT-IR spectrum the band observed at 486  $\text{cm}^{-1}$  is assigned to torsional mode of NH<sub>3</sub>. The bending of CO<sub>2</sub><sup>-</sup> is observed at 766  $\text{cm}^{-1}$ . Band at 929  $\text{cm}^{-1}$  is associated with CC-stretching vibration. Due to the stretching vibration involving carbon and nitrogen of the amino group there exists a peak at 1035  $\text{cm}^{-1}$ . The rocking of NH<sub>3</sub><sup>+</sup> structure is observed at 1183  $\text{cm}^{-1}$ . Bending vibrations of CH group are found in L-Threonine with peaks at 1246, 1314, 1341  $\text{cm}^{-1}$  in the spectrum. Bending vibrations of the CH<sub>3</sub> group is assigned to the peak at 1449  $\text{cm}^{-1}$ . The symmetric stretching of CO<sub>2</sub><sup>-</sup> structure is found at 1412  $\text{cm}^{-1}$  in the IR spectrum. The band at 1620  $\text{cm}^{-1}$  may be assigned to the asymmetric stretching CO<sub>2</sub><sup>-</sup>. The stretching vibrations also exist in both the NH<sub>3</sub><sup>+</sup> and CH structures. The symmetric stretching vibrations of NH<sub>3</sub><sup>+</sup> may be assigned to the vibration at 3023  $\text{cm}^{-1}$ . The asymmetric stretching of the NH<sub>3</sub><sup>+</sup> is observed at wave number 3150  $\text{cm}^{-1}$ .

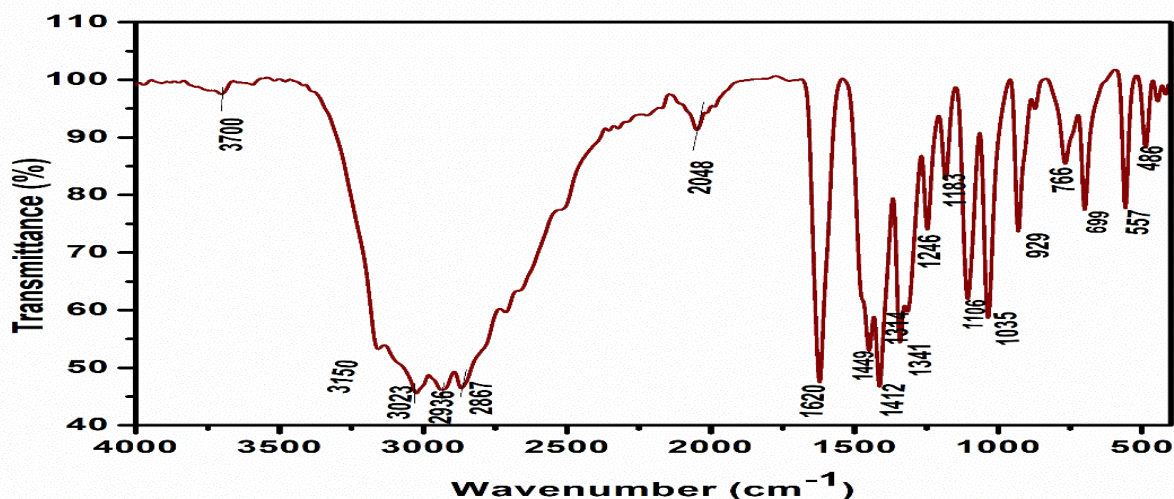


Fig. 2 FT-IR spectrum of L-Threonine

### 3.3 UV-Vis-NIR Spectral Analysis

The UV-Vis-NIR absorbance spectrum of the specimen was recorded using UV-Vis-NIR spectrophotometer region 200–1400 nm. The specimen of thickness about 1mm was used and recorded absorption spectrum is shown in Fig.3. From the graph, the lower cut off wavelength was observed at 232nm. Optical band gap energy was calculated and it is shown in Fig.4. The plot between energy ( $h\nu$ ) with  $(ah\nu)^{1/2}$  is made (where  $a$  is the absorption coefficient) and the optical band gap energy [7] is found to be 5.04 eV by extrapolating the slope region (where it cuts the X-axis). As a consequence of the wide bandgap, the grown crystal may be expected to possess high damage threshold [8].

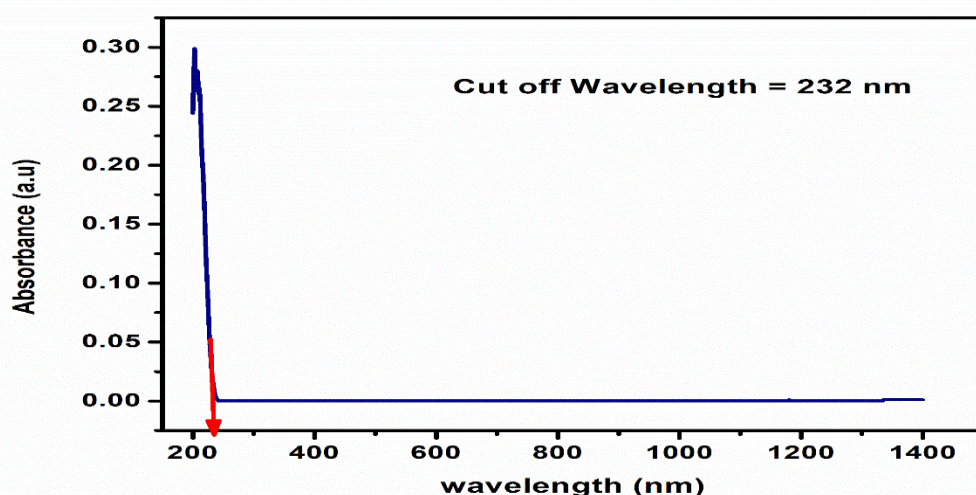
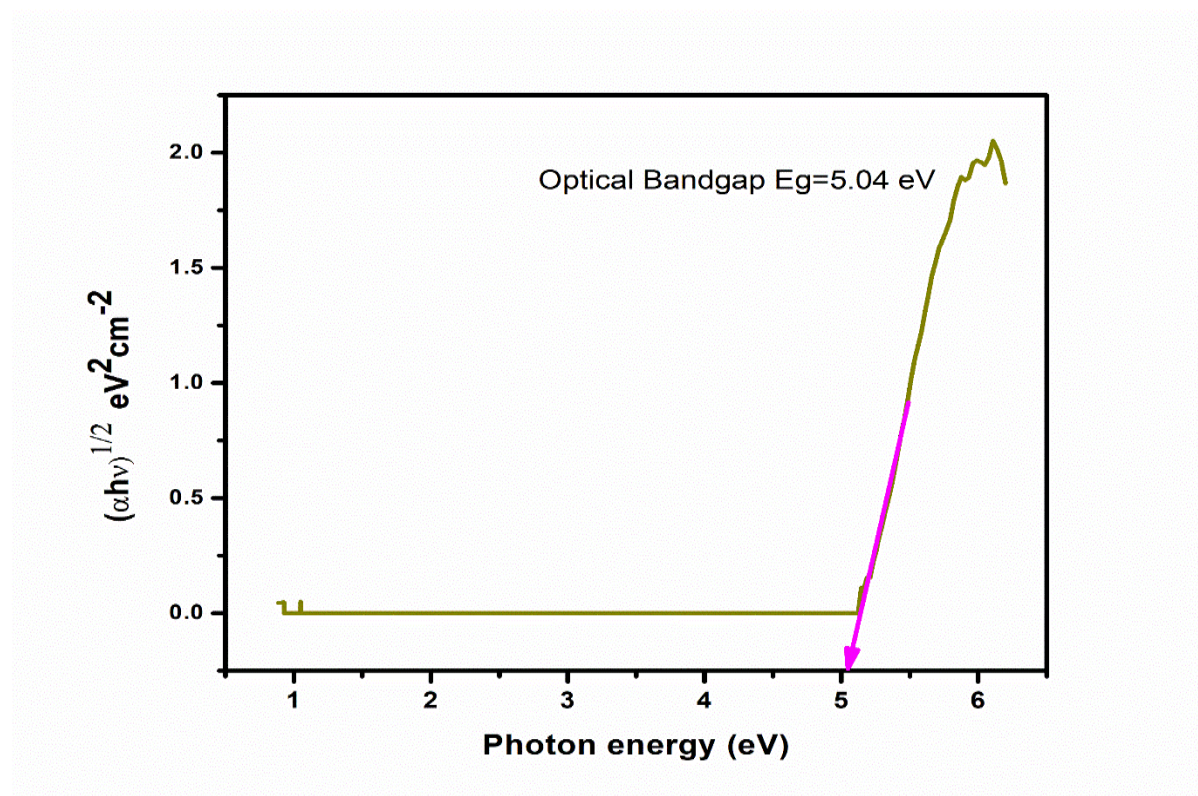


Fig. 3 UV-Vis-NIR absorbance spectrum of L-Threonine



**Fig. 4 Variation of photon energy ( $h\nu$ ) with  $(\alpha h\nu)^{1/2}$**

### 3.4 Absorption band tail (Urbach energy)

The optical absorption has a very important role in the field of material science which decides the suitability of a material for any optical applications. Because it gives the basic information about the optical band gap. The optical absorption spectra of the materials can be divided into three main regions; they are, Weak absorption region, which arises from defects and impurities present in the materials, Absorption edge region, which arise due to perturbation of structural and disorder of the system. The region of strong absorption that determines the optical band gap energy.

Along the absorption coefficient curve and near the optical band edge, there is an exponential part called as Urbach tail. This exponential tail appears to be more for poor crystalline materials which are disordered in lattices and for amorphous materials. If this tail appears to be minimum, this indicates good crystalline nature and also good perfection in lattice sites [9-11]. Near the optical band gap edge, the relationship between  $\alpha$  and energy of photons ( $h\nu$ ) is known as Urbach empirical rule, which is given by the following exponential equation (1) as follows,

$$\alpha = \alpha_0 \exp\left(\frac{h\nu}{E_U}\right) \quad (1)$$

where  $\alpha_0$  is a constant and  $E_U$  denotes the energy of the band tail or sometimes called Urbach energy. Taking the logarithm on both sides of equation (1), one can get an equation of straight line and it is given in equation (2) as follows,

$$\ln(\alpha) = \ln(\alpha_0) + \left(\frac{h\nu}{E_U}\right) \quad (2)$$

Therefore, the band tail energy or Urbach energy ( $E_U$ ) can be obtained from the reciprocal of the slope of the straight line obtained by plotting  $\ln(\alpha)$  against the incident photon energy ( $h\nu$ ). The value of  $E_U$  was found to be 0.118 eV, which is shown in Fig. 5.

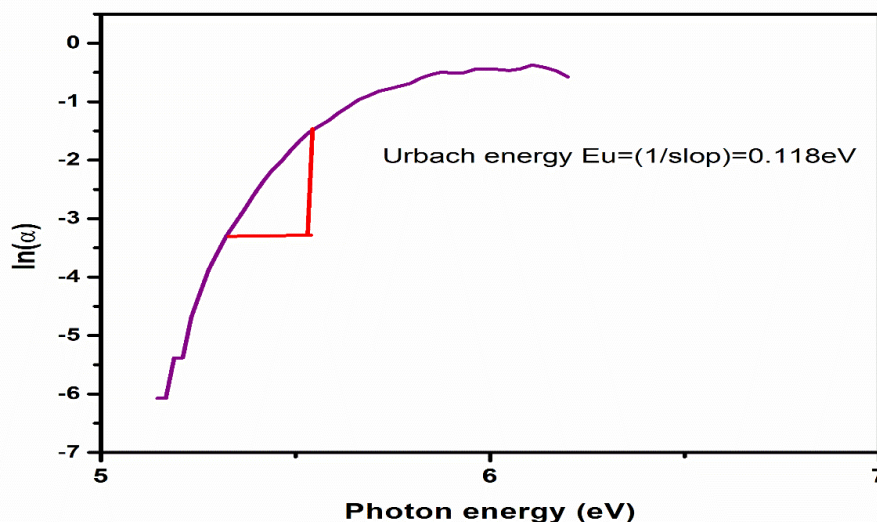


**Fig. 5 Plot of  $\ln(\alpha)$  vs Photon Energy ( $h\nu$ )**

From this value, the variation of optical band gap of the material is upto  $\pm 0.118$  eV. This minimum value of  $E_U$  indicates that the L-Threonine crystal has good crystallinity and also less disorder in near band edge. Moreover, Urbach suggested another relation for correlating both absorption coefficient ( $\alpha$ ) and the optical band gap energy using the equation (3),

$$\alpha = \beta \exp \left[ \frac{\sigma(h\nu - E_0)}{K_B T} \right] \quad (3)$$

where  $\beta$  is a pre-exponential constant and  $\sigma$  is another constant called the steepness parameter.  $E_0$  is the transition energy, which is equal to  $E_g$  for direct allowed transition. But for the indirect transition, it equals  $E_g \pm E_p$ , where  $E_p$  is the energy of the phonon, which is the main factor for affecting the band gap energy due to thermal dissociation of the lattice sites. L-Threonine crystal has direct band gap and hence  $E_0 = E_g$  and taking logarithm on both sides of equation (4) it can be rewritten in the following form

$$\left( \frac{h\nu}{E_U} \right) = \left( \frac{\sigma(h\nu)}{K_B T} \right) \quad (4)$$

Where,  $E_U$  is 0.118 eV,  $K_B$  is the Boltzmann constant ( $8.6173 \times 10^{-5}$  eV/K) and T is the absolute temperature (273.16 K). The steepness parameter ( $\sigma$ ) can be evaluated using following equation (5)

$$\sigma = \frac{K_B T}{E_U} \quad (5)$$

The value of  $\sigma$  was found to be 0.119. This is used for relating the strength of the electron-phonon interaction ( $E_{e-p}$ ), [12-13] which is calculated by using the following relation (6)

$$E_{e-p} = \frac{2}{3\sigma} \quad (6)$$

The strength of the electron-phonon interaction ( $E_{e-p}$ ) can be estimated and it was found to be 5.60. The wavelength of absorption edge (nm), optical band gap energy ( $E_g$ ), Urbach energy ( $E_U$ ), steepness parameter ( $\sigma$ ) and the electron-phonon interaction energy ( $E_{e-p}$ ) are given in Table 2.

**Table. 2 Urbach Energy of L-Threonine single crystal**

Description	Value
Wavelength of absorption edge (nm)	232 nm
Optical bandgap $E_g$	5.04 eV
Urbach energy $E_U$	0.118 eV
Steepness parameter $\sigma$	0.119
Electron-phonon interaction energy $E_{e-p}$	5.60

### 3.5 Determination of Optical Constants

The linear refractive index as a function of wavelength is crucial for developing NLO devices such as an electro-optic modulator, optical parametric oscillator and second harmonic generator. Large refractive index materials has lots of application in optoelectronic device fabrication such as advanced display systems, organic light emitting diodes (OLEDs), anti-reflecting coating, power lenses, dispersive prisms and image sensors etc. [14]. The refractive index of a material is depends on wavelength of incident light, lattice mismatch, crystal composition, carrier density and temperature [15]. Moreover, refractive index is vital to calculate the phase matching angles for NLO crystals [16]. The extinction coefficient (K) is obtained from the equation (7) given as

$$K = \frac{\alpha\lambda}{4\pi} \quad (7)$$

where  $\lambda$  is the wavelength of the incident radiation. The obtained extinction coefficient of the crystal with respect to photon energy are shown in Fig. 6.

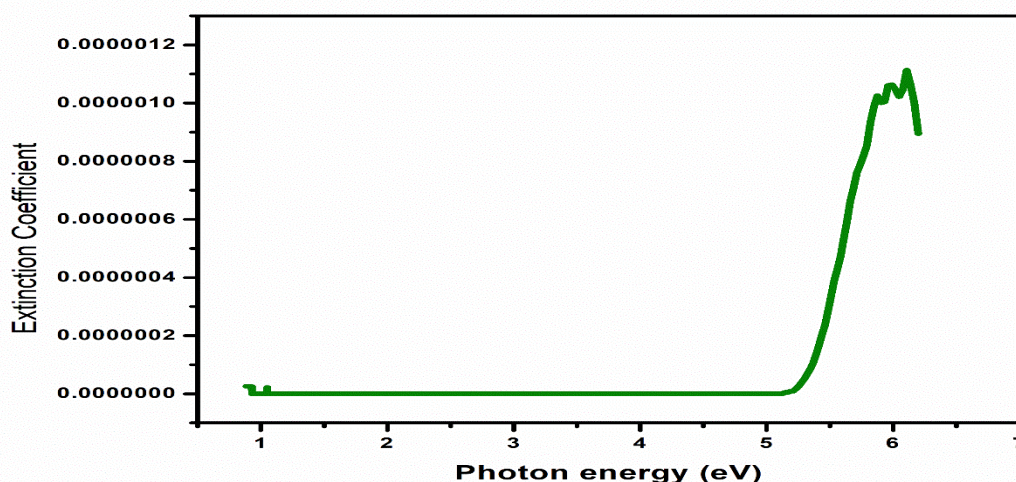


**Fig. 6 Plot of Photon Energy Vs Extinction Coefficient**

The refractive index ( $n$ ) was estimated by applying the following relation (8)

$$n = \frac{-(R+1) \pm \sqrt{(-3R^2+10R-3)}}{2(R-1)} \quad (8)$$

The graph between refractive index ( $n$ ) versus wavelength ( $\lambda$ ) is plotted and shown in the Fig. 7.

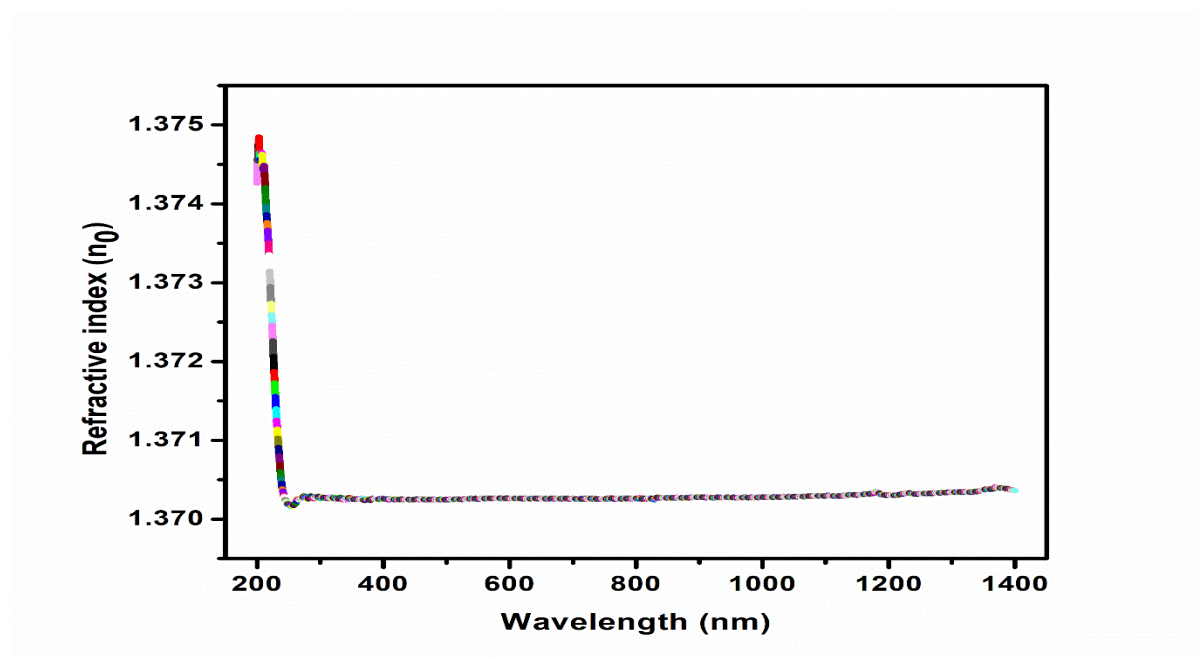


**Fig. 7 Wavelength dependence of Refractive indices ( $n_0$ )**

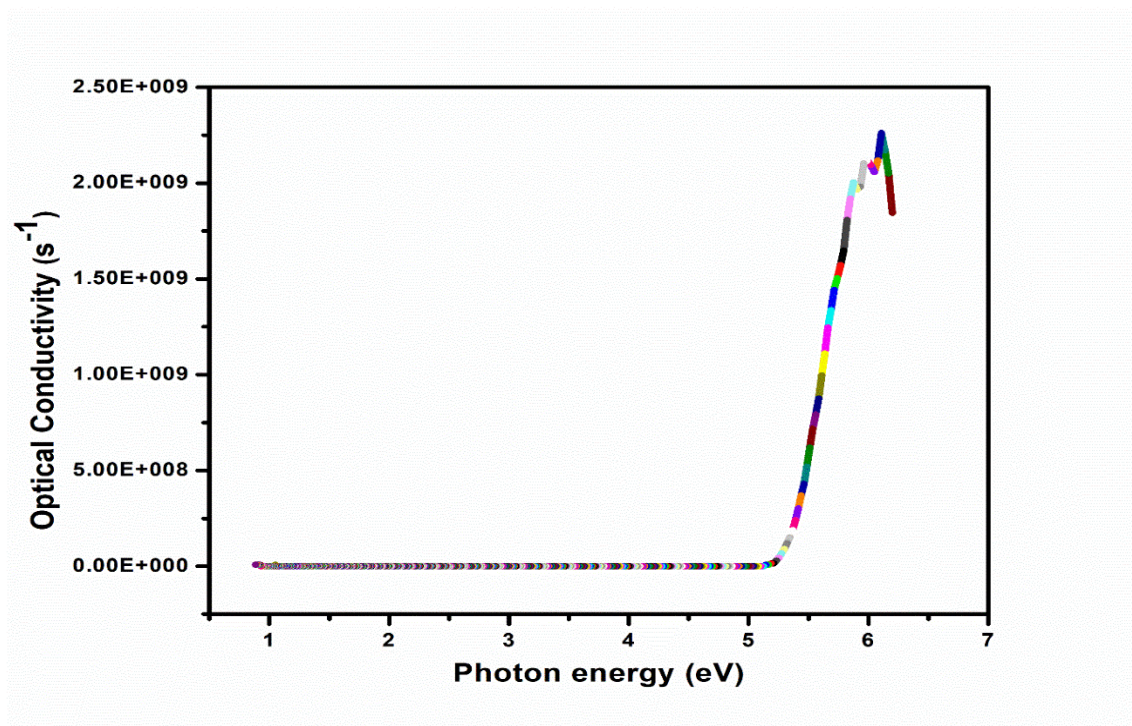
From the spectrum, linear refractive index was measured as 1.3702 at wavelength 257nm. The optical conductivity ( $\sigma_{op}$ ) [17] is a measure of the frequency response of the material when irradiated by light and it was calculated by using the relation(9).

Fig. 7 displays the optical conductivity versus photon energy of the grown crystal.

$$\sigma_{op} = \frac{\alpha n c}{4\pi} \quad (9)$$

where  $c$  is the velocity of light,  $\alpha$  is the absorption coefficient and  $n$  is the refractive index. Fig. 8 shows the variation of the optical conductivity as a function of photon energy for the L-Threonine crystal.





**Fig. 8 Optical Conductivity as a function of Photon Energy**

It can be seen clearly that the optical conductivity directly depends on absorption coefficient and the refractive index of the material. It is observed from the figure that optical conductivity increases sharply with increase in photon energy for title material under investigation. The increase in optical conductivity can be attributed to the increase in absorption coefficient.

L-Threonine shows high magnitude of optical conductivity confirms the presence of very high photo response nature of the material. This makes the material more prominent for device applications in information processing and computing.

### 3.5.1 Photoluminescence Studies

The photoluminescence emission spectrum of L-Threonine was recorded between 400 - 480nm using Jobin Yvon Spex spectrofluorometer. Fig. 9 shows the photoluminescence spectrum of the title material. A broad peak was observed in the range 400 - 475nm indicating that grown crystals has a blue fluorescence emission. It is clear from the spectrum states that strong PL emission of the title crystal confirms that the material has good structural perfection. The strong broad PL emission of the title material may find potential applications in optoelectronic devices [18]. This study infers newer materials for fluorescent lamps, X-ray image plates, dosimetry materials, lasing media, etc. [19–21]. Hence the photoluminescence studies confirm the suitability of the grown material has a blue fluorescence emission

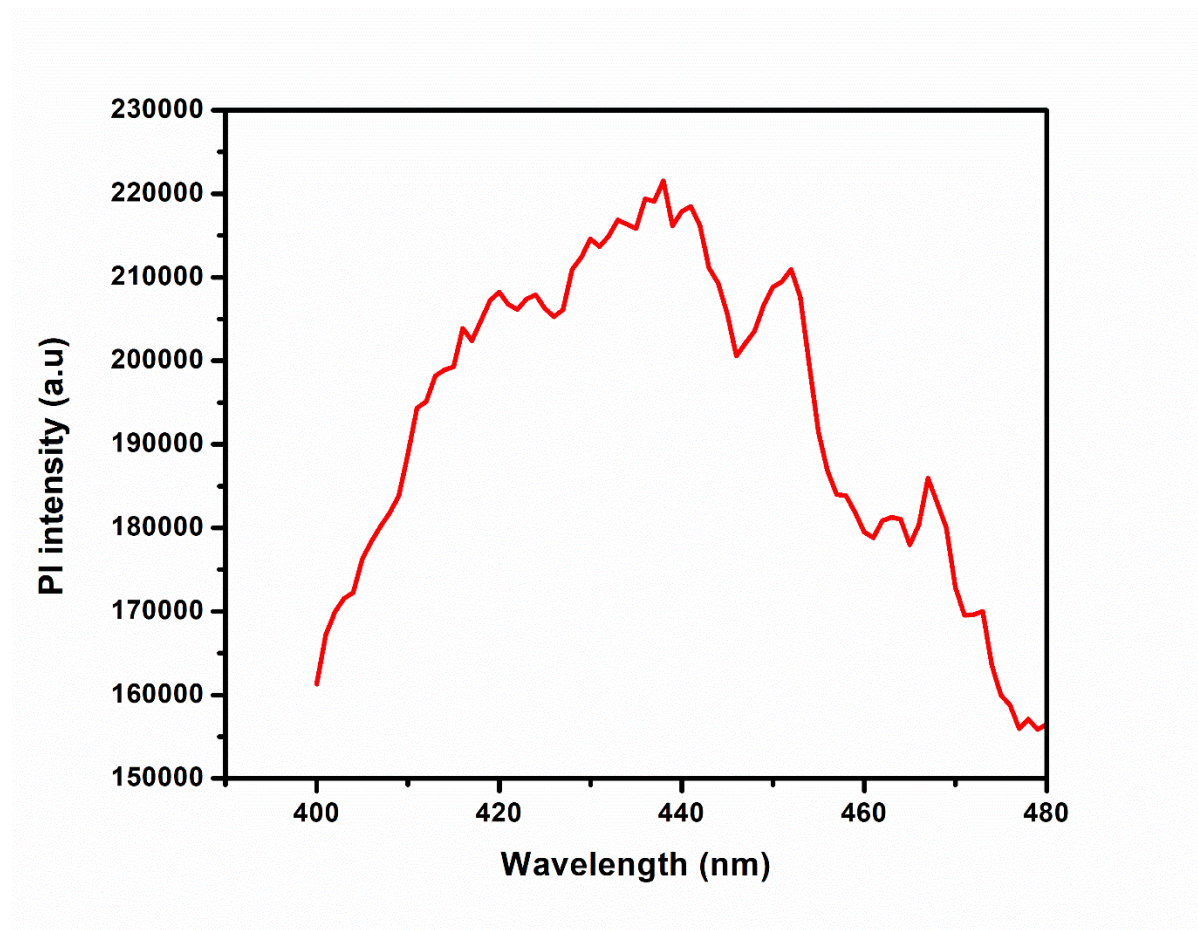
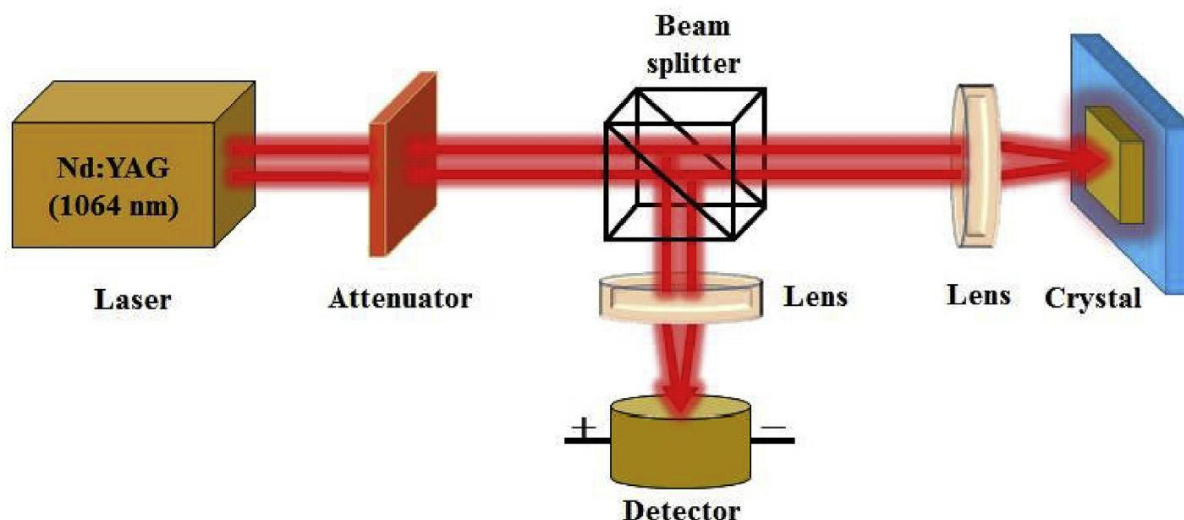


Fig. 9 Photoluminescence spectrum of L-Threonine

### 3.6 Laser Damage Threshold (LDT) Studies

For any nonlinear optical and laser applications, the laser damage threshold (LDT) value is an essential criteria for practical devices, because it gives the limit of performance in the optical system. For any applications, the materials must have ability to withstand for the given laser energy. But the materials may have laser induced bulk damage due to many reasons of intrinsic and extrinsic factors. Intrinsic damage limits the optical strength of materials that includes linear absorption, some nonlinear effects such as self-focusing, multi-photon absorption or two photons absorption, stimulated Brillouin scattering, stimulated Raman scattering, and electron avalanche break down. On the other hand, extrinsic damage includes material defects/voids, impurities and finished surface of materials. Also it affects the internal laser parameters such as pulse width, beam spot size, transverse and longitudinal laser modes and laser wavelength. Hence, the high optical surface damage tolerance is extremely important in the performance of nonlinear optical (NLO) and optoelectronic device applications [22].



**Fig. 10 Schematic diagram of LDT**

In the present study, the laser damage threshold value of L-Threonine crystal was measured using a Q-switched Nd: YAG (1064 nm) laser operating in transverse mode and pulse width of 6 ns in the frequency rate of 10 Hz. Fig.10 shows the Schematic diagram of LDT. Laser beam diameter of 1mm was used to irradiate on the well-polished L-Threonine crystal surface. The output laser beam was controlled with a variable attenuator and that crystal was placed at the focus of the converging lens of focal length 10 cm. During the laser irradiation, damage of the surface can be determined by the visual formation of damage and the input laser energy density was recorded by a power meter. The surface damage threshold of the grown crystal was calculated [23-24] using the following expression (10)

$$\text{Power density } P_d = \frac{E_p}{\tau \pi \omega_0^2} \quad (10)$$

The calculated laser damage threshold value of title material is 50.85 GW/cm<sup>2</sup>, which is compared to the some of the standard NLO materials [25-26] which is shown in the Table.3. It can be concluded that the grown crystal has good optical damage tolerance. Thus, the L-Threonine crystal is useful for high power laser applications

**Table. 3 Laser damage threshold value of L-Threonine with reported NLO crystals**

Crystal	Laser damage threshold (GW/cm <sup>2</sup> )	Reference
L-Threonine	50.85	Present work
L-arginine phosphate	10	[25]
L-alanine	16.41	[26]
Cobalt chloride doped L-alanine	26.53	[26]

### 3.7 Dielectric studies

The dielectric measurement is important for the analysis of electrical properties and defects in the materials [27]. This experiment was carried out, using cut and polished single crystal of L-Threonine as a dielectric medium. The silver paint was applied on the two surfaces. The

coated sample was placed for 10 min in a hot air oven at 40 °C for silver paste to tightly stick on both sides of the sample. This is beneficial for reducing air gaps between them to avoid external polarization by the air molecules. The surface of the sample has a good ohmic contact to the electrodes and without any short circuit condition. Then it was placed between two copper electrodes to form a parallel plate capacitor. The dielectric constant ( $\epsilon'$ ) of the grown L-Threonine crystal were studied as a function of frequency from 1 Hz to 1 MHz and it is shown in Fig. 11 respectively. From the plot, it is observed that the  $\epsilon'$  is relatively higher in the lower frequency region and it decreases further with an increase in the frequency. Normally  $\epsilon'$  of the material depends on the contributions of electronic, ionic, orientation and space charge polarizations. These polarizations are active in lower frequencies region. At higher frequency the  $\epsilon'$  becomes less due to significant loss of the polarizations [28]. The  $\epsilon'$  is calculated by the following relation (11) as follows,

$$\epsilon' = \frac{C_P d}{\epsilon_0 A} \quad (11)$$

where A is the area of cross-section of the sample, d is the thickness of the sample and  $\epsilon_0$  is the permittivity of free space ( $8.854 \times 10^{-12}$  F/m).

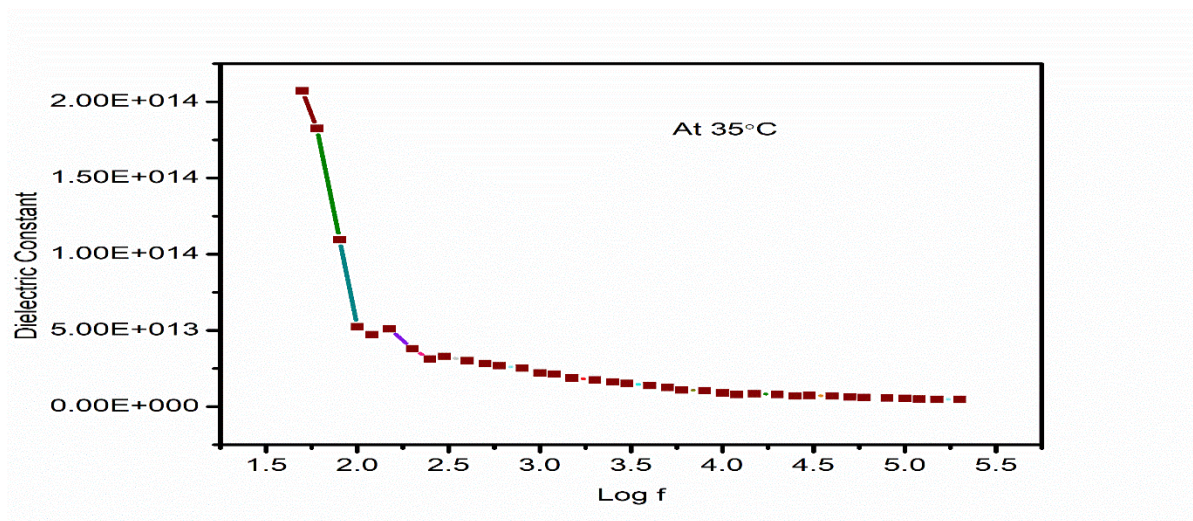


Fig. 11 Dielectric constant vs Log f

### 3.8 Electronic polarizability ( $\alpha$ )

The parameter of electronic polarizability ( $\alpha$ ) is essential for the efficiency of nonlinear materials. Theoretical calculation shows that the dielectric permittivity ( $\epsilon'$ ) depends on the valence electrons present in the given material's structure. The plasma energy, Penn gap energy, Fermi energy have been calculated and the electronic polarizability of the material was found out from the resultant values. The density of L-Threonine is calculated by using the following equation (12)

$$\rho = \frac{MZ}{N_A V} \quad (12)$$

where the molecular weight of the grown L-Threonine crystal is  $M=119.24$  g/mol, molecular unit cell  $Z=4$ ,  $N_A$  is Avogadro's number ( $6.023 \times 10^{23}$  mol $^{-1}$ ) and the volume of unit cell

$V=1.07 \times 10^{-21} \text{ cm}^3$ . The calculated density of grown crystal is  $1.4424 \text{ g/cm}^3$ . The valence electron plasma energy ( $\hbar\omega_p$ ) [29] is given by equation (13)

$$\hbar\omega_p = 28.8 \left( \frac{Z'x\rho}{M} \right)^{1/2} \quad (13)$$

where the total number of valence electrons of L-Threonine crystal is  $Z'=[(4 \times Z'_C) + (9 \times Z'_H) + (1 \times Z'_N) + (3 \times Z'_O)]=48$ . It can be calculated by substituting for each atom of C, H, N and O as the corresponding valence electrons are 4, 1, 5 and 6 respectively. According to the Penn model [29], the average Penn gap ( $E_P$ ) and Fermi energy ( $E_F$ ) [30] for L-Threonine are calculated using the following two relations (14 & 15)

$$E_P = \frac{\hbar\omega_p}{(\epsilon' - 1)^{1/2}} \quad (14)$$

$$E_F = 0.2947(\hbar\omega_p)^{4/3} \quad (15)$$

Then, the electronic polarizability ( $\alpha$ ) [31] of the grown crystal can be calculated by using the following relation (16)

$$\alpha = \left[ \frac{(\hbar\omega_p)^2 S_0}{(\hbar\omega_p)^2 S_0 + 3E_P^2} \right] X \frac{M}{\rho} X 0.396 X 10^{-24} \text{ cm}^3 \quad (16)$$

where  $S_0$  is a constant for a particular material which is given by using the relation (17)

$$S_0 = 1 - \left[ \frac{E_P}{4E_F} \right] + \frac{1}{3} \left[ \frac{E_P}{4E_F} \right]^2 \quad (17)$$

The value of electronic polarizability ( $\alpha$ ) [32] can be confirmed through the Clausius-Mossotti relation (18)

$$\alpha = \frac{3M}{\pi N_A \rho} \left[ \frac{\epsilon' - 1}{\epsilon' + 2} \right] \text{ cm}^3 \quad (18)$$

According to Maxwell relation, for visible light (high-frequency electric field), the  $\epsilon'$  is equal to the square of the linear refractive index ( $n_0$ ). The relationship between the electronic polarizability ( $\alpha$ ) and linear refractive index ( $n_0$ ) in such fields is described by the Lorentz-Lorenz equation [33] and it is calculated using equation (19)

$$\alpha = \frac{3M}{\pi N_A \rho} \left[ \frac{n_0^2 - 1}{n_0^2 + 2} \right] \text{ cm}^3 \quad (19)$$

The value of electronic polarizability ( $\alpha$ ) can also be obtained using the optical band gap, which is calculated using relation (20)

$$\alpha = \left[ 1 - \frac{\sqrt{E_g}}{4.26} \right] X \frac{M}{\rho} X 0.396 X 10^{-24} \text{ cm}^3 \quad (20)$$

where  $E_g$  is the optical band gap (eV) of the grown crystal. The coupled dipole method (CDM) was introduced by Renne and Nijboer [34-35]. In the CDM, each atom in a cluster is treated as a Lorentz atom (Drude oscillator), in which the electron is bound to the nucleus by a harmonic force. The atoms have no permanent electric dipole moment, but their dipole moments are to be induced by the applied local electric field. Naturally the electron is at a non-zero distance from the nucleus and hence the electron clouds are involving to induce electric dipole moments around the atoms. The electronic polarizability ( $\alpha$ ) of L-Threonine crystal was calculated [36] using the relation (21)

$$\alpha = \frac{Z'e^2}{m_e\omega_0^2} \quad (21)$$

where  $Z'$  is the total number of valence electrons, the charge of electron ( $e$ ) is  $1.602 \times 10^{-19}$  C and mass ( $m_e$ ) is  $9.1 \times 10^{-28}$  g and  $\omega_0$  is the natural frequency ( $2\pi f_0$ ),  $f_0$  is 1 MHz. The L-Threonine crystal has higher value of electronic polarizability ( $\alpha$ ) and these values are given in Table 4.

**Table. 4 Electrical properties of L-Threonine single crystal**

Electronic polarizability ( $\alpha$ )	Values of L-Threonine crystal
Plasma energy	21.92
Penn gap	2.8298
Fermi energy	18.43
Penn analysis	$1.048 \times 10^{-23}$
Clausius-Mossotti	$3.122 \times 10^{-23}$
Lorentz-Lorenz equation	$1.008 \times 10^{-23}$
optical band gap	$1.473 \times 10^{-23}$
coupled dipole method	$3.420 \times 10^{-23}$

### 3.9 Second Harmonic Generation (SHG) Analysis

The SHG efficiency of the title compound was determined using Kurtz–Perry powder technique [37]. A Q-switched Nd:YAG laser beam operating at 1064 nm, with an input energy of 0.70 J and pulse width of 6 ns with an input repetition rate of 10 Hz was used for this study. In order to confirm the NLO property the grown specimen was powdered with an average particle size range and filled in a micro-capillary tube of uniform bore and exposed to laser radiation. The output from the sample was monochromated to collect the intensity of 532 nm component. A sample of KDP powdered to the same particle size was used as reference material. Second harmonic generation from the sample was focused by a lens and detected by a photo multiplier tube. The SHG efficiency of the sample was compared with KDP and found to be comparatively 1.51 times greater than that of standard KDP. The second order nonlinear efficiency varies with the particle size of the powder sample [38].

#### Conclusion

Good quality optical single crystals of L-Threonine were grown by slow evaporation solution technique at ambient temperature. Single crystal X-ray diffraction study reveals that the grown crystal belongs to orthorhombic system. Functional groups were identified by using FT-IR spectrum. UV-Vis-NIR studies were carried out and the lower cut-off wavelength was observed at 232 nm and the optical bandgap was found to be 5.04 eV. The minimum of Urbach energy indicates that the grown crystal has good crystalline perfection. The optical parameters such as the absorption coefficient ( $\alpha$ ), extinction coefficient ( $K$ ) and refractive

index ( $n_0$ ) were analyzed with respect to the wavelength. The laser damage threshold value was tested and it was  $50.85 \text{ GW/cm}^2$  for 1064nm wavelength of Nd:YAG laser radiation. The higher value of surface laser damage threshold of L-Threonine suggests that these crystals may have a favorable application in laser frequency conversion. The dielectric permittivity of L-Threonine crystal was measured as a function of frequency. The electronic polarizability ( $\alpha$ ) of L-Threonine crystal was calculated by fundamental parameters like plasma energy, Penn gap, Fermi energy using dielectric permittivity and it is in good agreement with the values obtained from Clausius-Mossotti relation, Lorentz-Lorenz equation, optical band gap energy and CDM. The second harmonic generation was tested by Kurtz-Perry powder technique and efficiency was compared with standard KDP.

### **Acknowledgements**

The authors are acknowledged to SAIF, IIT-Madras, Chennai – 600 036 for the data collection of single crystal X-ray diffraction. The authors extend their acknowledgment to B.S. Abdur Rahman Crescent Institute of Science & Technology, Chennai - 600 048 for data collection of FT-IR, UV-Vis-NIR, Photoluminescence, Second Harmonic Generation and Laser Damage Threshold studies.

### **References**

- [1] D. S. Chemla and J. Zyss, *Nonlinear Optical Properties of Organic Molecules and Crystals*, Academic Press, New York, NY, USA, 1987.
- [2] R. A. Hann and D. Bloor, Eds., *Organic Materials for Nonlinear Optics*, Royal Society of Chemistry, London, UK, 1989.
- [3] M. H. Lycons, Ed., *Materials for Nonlinear Optics and Electro-Optics*, vol. 103 of Institute of Physics Conference Series, Institute of Physics, Bristol, UK, 1989.
- [4] R.W. Boyd, *Nonlinear Optics*, Academic Press, San Diego, 1992.
- [5] B.E. Saleh, M.C. Teich, *Fundamentals of Photonics*, Wiley, New York, 1991
- [6] D.P. Shoemaker, J. Donohye, V. Shoemaker, R.B. Corey, *J. Am. Chem. Soc.* 72 (1950) 2328-2349
- [7] Hou Wenbeo, Yuan Duorong, Xu Dong and Jiang Minhua, *J. Cryst. Growth* 133 (1993) 71-74.
- [8] M.D. Shirsat, S.S. Hussaini, N.R. Dhumane, V.G. Dongre, *Cryst. Res. Technol.* 43 (2008) 756-761.
- [9] S.J. Ikhmayies, R.N. Ahmad-Bitar, *J. Mater. Res. Technol* 2 (2013) 221–227.
- [10] K.A. Aly, A.M. Abd Elnaeim, M.A.M. Uosif, O. Abdel-Rahim, *Physica B: Condensed Matter* 406 (2011) 4227–4232.
- [11] F. Urbach, *Phys. Rev.* 92 (1953) 1324.
- [12] M. Karimi, M. Rabiee, F. Moztarzadeh, M. Tahriri, M. Bodaghi, *Curr. Appl. Phys.* 9 (2009) 1263-1268.
- [13] J.X. Wang, S.S. Xie, H.J. Yuan, X.Q. Yan, D.F. Liu, Y. Gao, Z.P. Zhou, L. Song, L.F. Liu, X.W. Zhao, X.Y. Dou, W.Y. Zhou, G. Wang, *Solid State Commun.* 131 (2004) 435–440
- [14] J. Liu, M. Ueda, *J. Mater. Chem.* 19 (2009) 8907
- [15] B. Broberg, S. Lindgren, *J. Appl. Phys.* 55 (1984) 3376

- [16] F. Koohyar, J. Thermodyn. Catal. 4 (2013) 1000e117
- [17] R. Hanumantharao, S. Kalainathan, G. Bhagavannarayana, Spectrochim Acta Part A 91 (2012) 345-351
- [18] G. Blasse, B.C. Grabmaier, Luminescent Materials, Springer, New York, 1994.
- [19] C.R. Ronda, J. Alloys Compd. 225 (1995) 534–538.
- [20] Y.W. Tan, C.S. Shi, J. Solids State Chem. 150 (2000) 178–182.
- [21] G.H. Sun, G.H. Zhang, Z.H. Sun, X.Q. Wang and D. Xu, Mater. Chem. Phys. 127 (2011) 265–270.
- [22] R.M. Wood, “Laser-induced Damage of Optical Materials”, Institute of Physics Publishing, Dirac House, Bristol, UK, (2003).
- [23] P. Karuppasamy, V. Sivasubramani, M. Senthil Pandian and P. Ramasamy, RSC Adv 6 (2016) 109105–109123.
- [24] V. Venkataramanan, G. Dhanaraj, B. R. Prasad, C. K. Subramanian & H. L. Bhat, Ferroelectrics, 155 (1994) 13-18,
- [25] Anuj Krishna, N. Vijayan, Shashikant Gupta, Kanika Thukral, V. Jayaramakrishnan, Budhendra Singh, J. Philip, f Subhasis Das, K. K. Mauryab and G. Bhagavannarayanab., RSC Adv., 4 (2014) 56188–56199
- [26] Cicili Ignatius, S. Rajathi, K. Kirubavathi and K. Selvaraju., J. Nonlinear Optic. Phys & Mat. 25 (2016) 1650017
- [27] D. Xue, K. Kitamura, Solid State Commun 122 (2002) 537–541.
- [28] C. Balarew, R. Duhlew, J. Solid-State Chem. 55 (1984) 1–6
- [29] J.D. Jackson, Classical Electrodynamics, Wiley Eastern, 1978, p. 321.
- [30] D.R. Penn, Phys. Rev. 128 (1962) 2093–2097.
- [31] N.M. Ravindra, V.K. Srivastava, J. Infrared Phys. 20 (1980) 67–69.
- [32] P.V. Rysselberghe, J. Phys. Chem. 36 (1932) 1152–1155.
- [33] M. Born, E. Wolf, Osnovy Optiki, second ed., (1973) Moscow.
- [34] M.J. Renne, B.R.A. Nijboer, Chem. Phys. Lett. 1 (1967) 317–320.
- [35] B.R.A. Nijboer, M.J. Renne, Chem. Phys. Lett. 2 (1968) 35–38.
- [36] B.W. Kwaadgras, M. Verdult, M. Dijkstra, R. van Roij, J. Chem. Phys. 135 (2011) 134105
- [37] S.K. Kurtz, T.T. Perry, J. Appl. Phys. 39 (1968) 3798–3813.
- [38] M. Parthasarathy, R. Gopalakrishnan, Spectrochim. Acta A, 97 (2012) 1152-1158